RSC Advances

ROYAL SOCIETY OF CHEMISTRY

www.rsc.org/advances

Self- assembled supramolecular structure of *N,N,N′,N′*-tetramethylethylenediammonium-bis-(4-nitrophenolate):synthesis, single crystal growth and photo physical properties

P. Nagapandiselvi[a], C. Baby[b] and R. Gopalakrishnan[a]*

[a]*Crystal Research Lab, Department of Physics, Anna University, Chennai, India.*

[b]*Sophisticated Analytical Instrument Facility, Indian Institute of Technology Madras, Chennai, India.*

Abstract

The synthesis, growth and structure of a novel organic third order nonlinear optical (NLO) crystal namely, *N,N,N′,N′*-tetramethylethylenediammonium-bis(4-nitrophenolate) (TMEDA4NP) is presented. The solubility of the compound in methanol and acetonitrile solvents is compared and the growth condition was optimized. Single crystals of TMEDA4NP were grown in acetonitrile solvent using slow evaporation technique at 303K. The crystal structure elucidated from single crystal X- ray diffraction analysis at 293K showed that the title compound crystallizes in monoclinic crystal system with space group $C_2/_C$. The molecular structure was further confirmed by modern spectroscopic techniques like FT-IR, FT-NMR, UV-Vis-NIR and Fluorescence. The transparency in the visible region and hence the feasibility of the crystal for NLO applications was established from UV-Vis-NIR study. Fluorescence emission of the crystal also revealed that the title compound can serve as a photoactive material. The protonation of TMEDA4NP was unambiguously confirmed from the NMR data. Thermo gravimetric analysis (TGA) showed that TMEDA4NP was thermally stable up to 110 °C. The mechanical strength of the crystal was assessed by Vickers Microhardness tester. Etching studies were carried out on (100) plane of the as grown surface of the crystal. Third order susceptibility was measured using z scan technique by employing picosecond Nd-YAG laser indicates that the title compound can serve as a promising candidate for third order NLO applications.

***Keywords*:** Nonlinear optical crystal, Growth from solution, X-ray Diffraction, supramolecular structure, N,N,N′,N′-tetramethylethylenediammonium-bis-(4-nitrophenolate).

*Corresponding author. Tel.: +91-44-2235 8710/ +91-44-2235 8707. Fax: +91-44-2235 8700
Email.: krgkrishnan@annauniv.edu, krgkrishnan@yahoo.com (R. Gopalakrishnan)

1. Introduction

Recent developments in ultrafast signal processing are attributed mainly to the materials possessing higher order nonlinear optical susceptibility which is originated from the higher order nonlinearity.[1-3] In this context, organic nonlinear optical (NLO) materials have captured much attention in the recent past due to their relatively higher nonlinearity and fast response. Notable advantages of organic NLO systems over inorganic counterparts include their high electronic susceptibility through high molecular hyperpolarizability and facile modification through standard synthetic methods.[4-7] It is also feasible to fine tune the chemical structure and properties of organic NLO materials for specific applications such as optical switching, power limiting for sensor protection and optical computing.[8,9]

Investigation of organic NLO compounds are generally based on the nature of both electron-donor and electron-acceptor substituents leading to the charger transfer process.[10] The quest also depends on the growth of crystals containing organic ions, which in turn favors polarization of the π electrons in its counterparts for developing NLO chromophores possessing high nonlinearity, good thermal and mechanical stability.[11,12] In this scenario, analysis by an acid-base approach gives an efficient result for designing such donor-acceptor systems.[13,14] Crystallization of organic solids with acidic and basic characteristics is often controlled by the difference in pKa values of precursor components.[15] If the difference between pKa is greater

than three, salts of the compound could be formed and the architecture of molecular species for desired applications can be made quite easy. On the other hand, if the difference is less than three, the force which controls the crystalline environment cannot be easily predictable and often packed as a self-assembled one.[16-18] The growth of single crystals from such compounds is dominated by both hydrogen bonding and minute dipole–dipole interactions which determines the physical properties of the compound.[19] It is reported that the para substituted donor-acceptor systems are holding high delocalized electrons for nonlinear optical applications.[20] 4-nitrophenol being one such compounds, with donor-acceptor π systems in its counterparts, aid to engineer new molecules for NLO applications.[21] However, it acts as an acid donor (pKa-7.16) when reacts with bases resulting in the formation of salts. Careful selection of acceptor (base) helps to extend the π electrons in its sub chain for increasing its nonlinearity. In this aspect, *N,N,N′,N′*-tetramethylethylenediamine (TMEDA, pKa = 8.97) is an interesting candidate since it is a strong base and a double acceptor system with the possibility of adopting layer structure when reacting with 4-nitrophenol, resulting in the formation of well delocalized, *N,N,N′,N′*-tetramethylethylenediammonium-bis-(4-nitrophenolate) (TMEDA4NP). Molecules with these features generally crystallize in non-centrosymmetrical fashion and favors second order nonlinear optical properties.[22] In this paper, we report the results of a detailed systematic investigation about the nature of crystallization, self assembled structure and the order of nonlinearity of TMEDA4NP crystals; from synthesis to the structure-property relationship.

2. Experimental Procedures

2.1 Synthesis of TMEDA4NP

TMEDA4NP was synthesized by mixing analytical grade (purity 98%) 4-nitrophenol and *N,N,N′,N′*-tetramethylethylenediamine (TMEDA) in the ratio 2:1 in methanol medium at room temperature. Yellow precipitate was formed within few seconds on mixing the TMEDA in to 4-nitrophenol. The resultant product was analyzed by thin layer chromatography (TLC). The reaction mechanism of the synthesis of TMEDA4NP is depicted in Scheme 1.

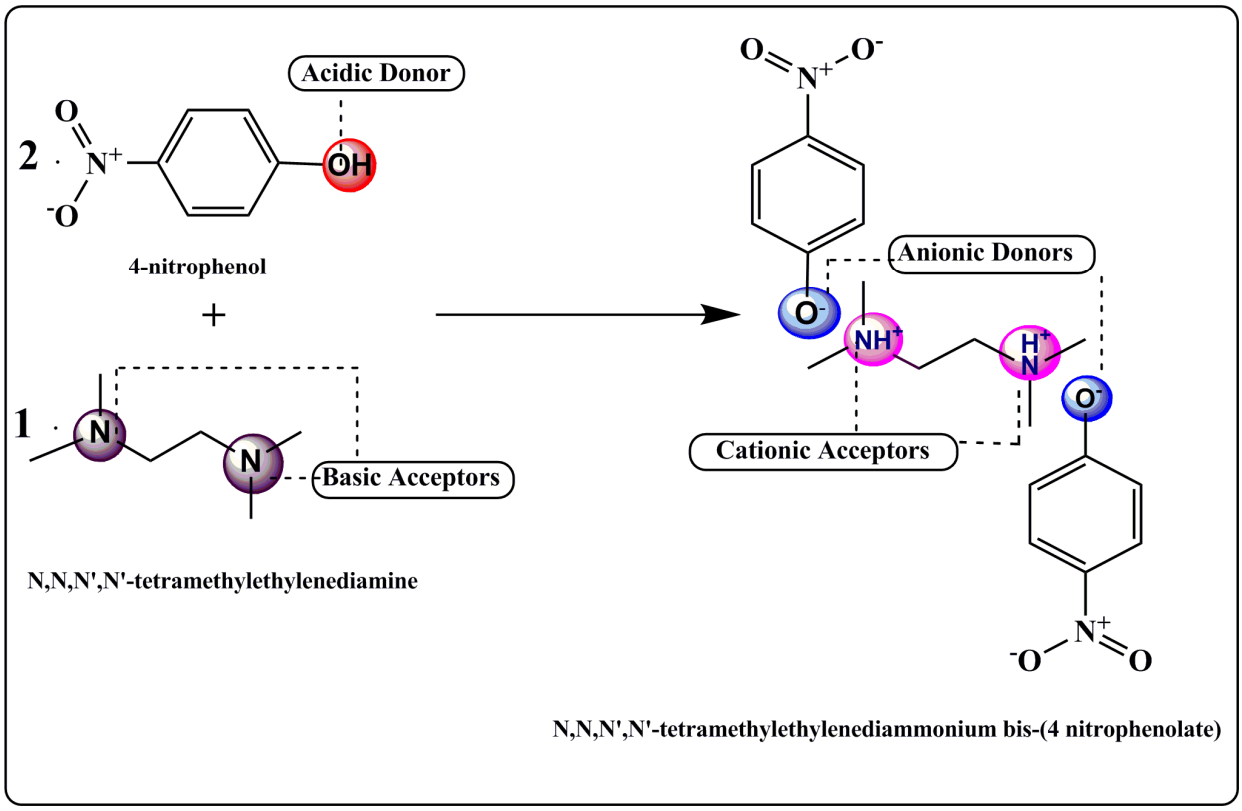

Scheme 1: Formation of TMEDA4NP

2.2 Estimation of Solubility and pH of Solution

Solvent selection is one of the important criteria to optimize the growth conditions for growing good quality single crystals.[23] The solubility of TMEDA4NP was estimated gravimetrically in methanol and acetonitrile solvents for five different temperatures (30, 35, 40, 45 and 50°C) (†ESI 1.1). The pH of the solution was also measured at the above mentioned

temperatures and is tabulated in Table 1. A graph is then plotted between temperature and concentration of the solute and is shown in Fig. 1. From the graph it is observed that the solubility of TMEDA4NP increases with increase in temperature (positive solubility gradient) in both solvents. A notable feature of the solubility graph is that the solubility of TMEDA4NP in methanol medium is higher than that of acetonitrile. Also the pH of the solution prepared in methanol medium was found to be higher than that in acetonitrile at all temperatures. This could be attributed to the polarity difference of solvents and also the difference in pH values.

Table 1. Variation of pH of the growth solution at different temperatures

Temperature (^{o}C)	pH	
	Methanol	Acetonitrile
25	9.15	8.99
30	9.07	8.79
35	8.97	8.69
40	8.84	8.47
45	8.73	8.30
50	8.64	8.15

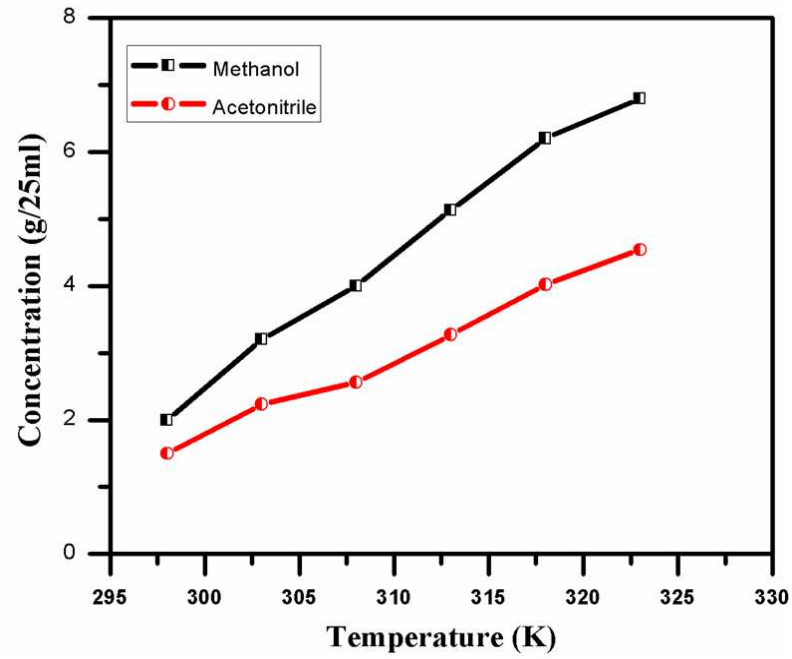

Fig. 1 Solubility of TMEDA4NP in different solvents

2.3 Crystal Growth

For nonlinear optical applications, the growth of bulk single crystals with superior optical qualities has been the subject of interest.[23] Due to relatively higher solubility and pH of TMEDA4NP in methanol than in acetonitrile; the crystal growth was attempted only in acetonitrile solvent. TMEDA4NP was dissolved in acetonitrile solvent and magnetically stirred for 4 hours to maintain homogeneity. The resultant solution was then filtered using Whatmann 41 filter paper and kept in a constant temperature bath (CTB) at 35 ºC for slow evaporation. Spurious nucleation was observed during the crystallization process. The fast crystallization of the title compound can be better understood from the layer crystal structure obtained as described *vide infra.* The synthesized material was recrystallized repeatedly (five times) to purify the compound and the melting point of the material was checked every time after recrystallization.

The melting point of the final purified compound was found to be 118 ºC. A well purified TMEDA4NP obtained from the recrystallization is used for the growth.

The crystal growth generally depends on the supersaturation ratio (driving force for crystallization) and the pH of the solution.[24] Higher the supersaturation ratio, there is less hindrance in the growth of the crystal. However; the size of the crystal is often restricted, owing to the fact that there is spurious nucleation.[25] Initially, a supersaturated solution was prepared at 35, 40 and 45 ºC. The temperature was raised at an increment of 5 ºC for attaining the saturated state and then allowed for controlled evaporation. Finally, a single crystal of $30 \times 24 \times 5$ mm^3 was harvested within 10 days from the mother solution at 40 ºC and maintaining at a pH of 8.47. However, for solutions kept for evaporation at other two temperatures (45°C and 50°C), there were only spurious nucleation. This could be because of the faster solvent evaporation at higher temperatures. The harvested crystal of TMEDA4NP is shown in Fig. 2(a) and its predicted morphology is given in Fig. 2(b).

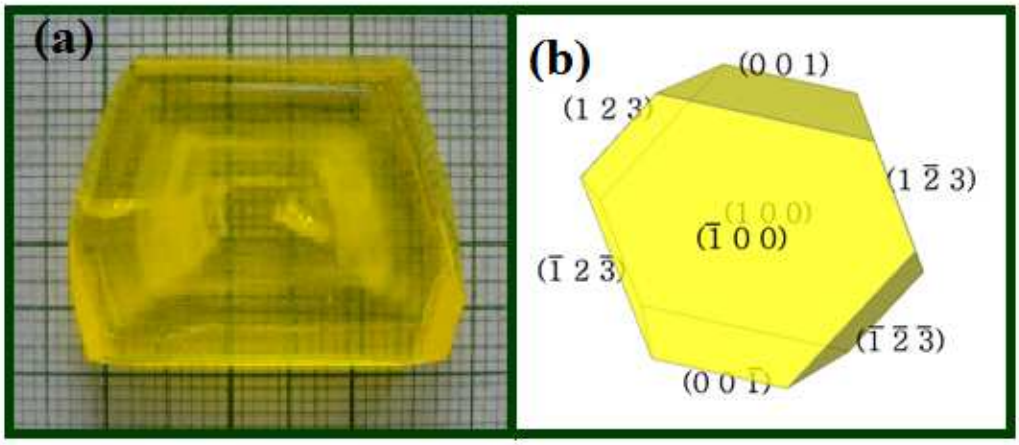

Fig. 2(a) Harvested crystal of TMEDA4NP **(b)** Predicted morphology

2.4 Characterization Studies

The crystal structure of TMEDA4NP was determined using Bruker AXS Kappa APEX II single crystal X ray diffractometer equipped with graphite-monochromated MoKα radiation (λ=0.71073Å) at room temperature. A single crystal of dimension 0.35 × 0.3 × 0.25 mm^3 was used for diffraction analysis. Accurate unit cell parameters were determined from the reflections of 36 frames measured in three different crystallographic zones, using the method of difference vectors. The data collection, data reduction and absorption correction were performed by APEX2, SAINT-plus and SADABS programs.[26] The structure was solved by direct methods and the non-hydrogen atoms were subjected to anisotropic refinement by full-matrix least squares on F^2 using SHELXL-97 program.[27] The positions of all the hydrogen atoms were identified from the difference electron density map and they were constrained to ride on the corresponding non-hydrogen atoms. The Cambridge Crystallographic Data Centre (CCDC No.: 900636) contains the supplementary crystallographic data. The Morphology of the crystal was simulated from the CIF File using WinXMorph software.

The FT-IR Spectrum was recorded on a Bruker OPTIK 500200 spectrometer in the frequency range of 4000 - 450 cm^{-1}, using KBr pellet method. FT-NMR spectra were recorded in CD_3CN solvent on a Bruker Avance III 500 MHz instrument, using TMS as an internal reference standard. Gradient enhanced 2D COSY and HSQC spectra were recorded using the standard pulse programs from Bruker. The UV-VIS-NIR spectrum of TMEDA4NP crystal with thickness of 2 mm was recorded using Perkin Elmer Lambda 35 UV-VIS spectrometer. The fluorescence spectrum of TMEDA4NP single crystal was recorded using a Jobin Yvon Fluorolog -3-11 Spectrofluorimeter. The thermal stability of the TMEDA4NP was analyzed using the NETZSCH STA 449F3 series Simultaneous Thermal Analyzer. The phase transition

was studied using NETZSCH DSC 204C Differential Scanning Calorimeter. The hardness of the crystal was assessed by MATSUZAWA MMTX Vickers's microhardness tester attached to an optical microscope and the experiment was carried out at room temperature. Static indentations of diamond pyramidal intender were made on (100) plane of selected smooth and flat surface of the crystal with various loads of different magnitude such as 5, 10,15, 20, 25 and 30g by keeping the dwell time as 10s for each indentations and the diagonal length of each indention was measured. In order to avoid the surface effect on the crystal, the distance between the successive indentations was increased four times with respect to the diagonal length of the previous indentation mark. Etching studies were made on the (100) plane of as grown TMEDA4NP crystals using acetonitrile as an etchant and the etched surface was viewed through optical microscope in the reflection mode.

The experimental setup used for the open aperture Z scan is described elsewhere.[28] A well cut defect free crystal of thickness 2 mm was used for the study. The second harmonic (532 nm) of a picosecond Nd:YAG laser (Continuum Model YG601, 40 ps, 10 Hz) was employed. The beam waist (ω_o) of the Gaussian laser pulse at focus is 24 μm and the corresponding Rayleigh range (Z_R) is 3.4 mm. It also satisfies the thin sample approximation condition (i.e., $Z_R >> L$, where L is the thickness of the sample). The crystal was mounted on the translation disk and moved along the focal plane of 50 mm double convex lens. The entire output transmitted light from the sample collected with a big aperture double convex lens of focal length of 200 mm at a far field and detected with help of the photo detector containing Becker and Hickle, PDI-400 photo diode. The irradiance dependence of the Z-scan profiles of TMEDA4NP crystal was recorded at wavelength of 532 nm.

3. Results and Discussion

3.1 Single crystal X ray diffraction analysis

From the single crystal X-ray diffraction analysis, it is clear that the title compound crystallizes in monoclinic space group C2/c. The asymmetric unit comprises of one half of *N,N,N′,N′*-tetramethylethylenediammonium dication and one 4-nitrophenolate anion constituting 1:2 molecular ratio. In the crystal structure, TMEDA dication and 4-nitrophenolate anion have self-assembled themselves to form a supramolecular structure. The symmetry equivalence used to generate the molecular system is -x+2, -y, -z+2. The ORTEP diagram of the TMEDA4NP is shown in Fig. 3. The 4-nitrophenolate anion is almost planar showing normal geometrical parameters. Due to high electronegativity of the oxygen, it acts as an acceptor for the formation of N-H…O and O-H…O hydrogen bonds which constitute the molecular network in the system. The H2A at N2 forms a strong N2 -H2A…O3 hydrogen bond between the anions and cations in the system as shown in Fig.4. These molecular ions are interlinked through weak C-H…O hydrogen bonds C9-H9B…O2, C8-H8B…O3 and C9-H9C…O1. The inversion related anions and cations are linked through N2-H2A…O3 and C8-H8B…O3 hydrogen bonds to form a R_4^2 (10) motif to generate one dimensional network along [010] direction (†Fig.S1). These [010] networks are further interlinked through other C-H…O hydrogen bond generating a three dimensional network of anions and cations. The crystallographic data of TMEDA4NP is tabulated in Table 2 and some selected bond lengths and bond angles are listed in †Table S1. The hydrogen bonds present in TMEDA4NP are presented in †Table S2.

In the molecular system, the *N,N,N′,N′*-tetramethylethylenediaminium dication and one 4-nitrophenolate anion are alternatively stacked along (100) plane. The benzene planes of the

4-nitrophenolate anions are inclined to an angle of 60.66º with respect to the (100) plane and offer weak ionic forces and hydrogen bonding interactions, which can significantly contribute to lowering of lattice enthalpy.[29] This ultimately provides the driving force for the coexistence of both amine cations and phenolate anions together in the crystal. Such forces can also induce fast crystallization. The crystal structure of TMEDA4NP is comparable with that of potassium 4-nitro phenolate. However, in potassium 4-nitrophenolate,[30] potassium ion is located close to nitro group while in TMEDA4NP crystal, the protonated amine is close to the phenolic oxygen. The phenolic groups in TMEDA4NP are oppositely oriented with respect to each other to minimize repulsion. In order to acquire such orientation, the assistance comes from protonated amines. The reason for the three phenolic ions together in a group is rather difficult to unravel, but it could be plausible that more than three phenolic ions lead packing problem, while less than three will lower the enthalpy, which eventually favors the fast crystallization.

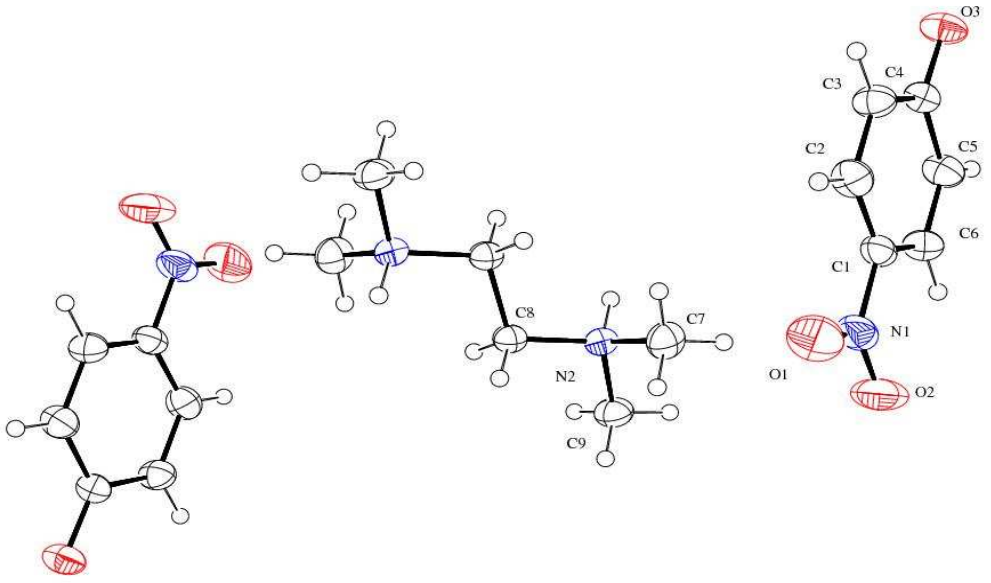

Fig. 3 ORTEP diagram of TMEDA4NP

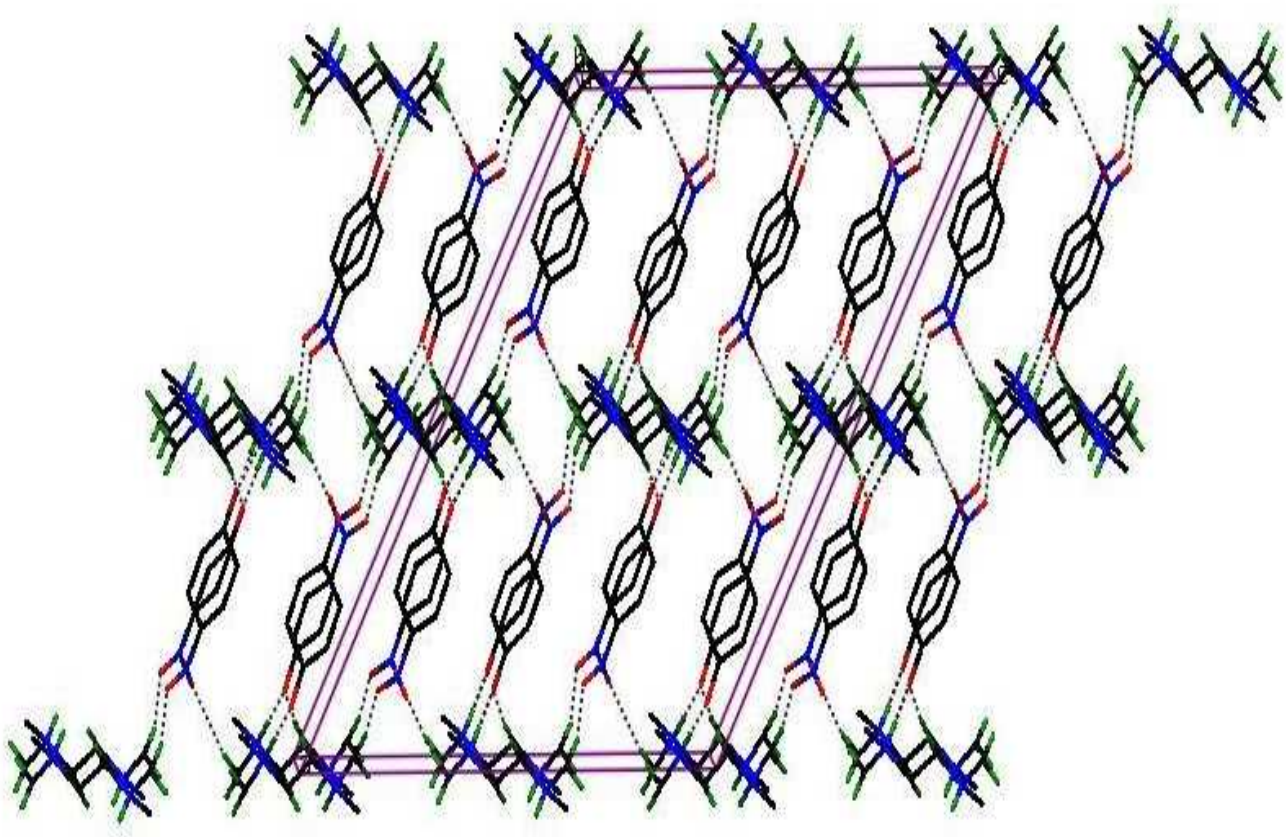

Fig. 4 Packing of TMEDA4NP along b axis

Table 2. Crystallographic data of TMEDA4NP

Identification code	TMEDA4NP
Empirical formula	C18 H26 N4 O6
Formula weight	394.43
Temperature	293(2) K
Wavelength	0.71073 Å
CCDC No	900636
Crystal system, space group	Monoclinic, C_2/c
Unit cell dimensions	a = 23.051(5) Å α = 0.000(5)°.
	b = 5.624(5) Å β = 121.026(5)°.
	c = 17.451(5) Å γ = 90.000(5)°.
Volume	1938.7(19) $Å^3$
Z, Calculated density	4, 1.351 mg/m^3
Absorption coefficient	0.102 mm^{-1}
Theta range for data collection	2.43 to 28.10°.
Limiting indices	-30<=h<=30, -7<=k<=7, -23<=l<=23
Reflections collected / unique	10639 / 2366 [R(int) = 0.0271]
Completeness to theta	28.10 , 99.8 %
Max. and min. transmission	0.9748 and 0.8950
Refinement method	Full-matrix least-squares on F^2
Goodness-of-fit on F^2	1.025
Final R indices [I>2sigma(I)]	R1 = 0.0428, wR2 = 0.1130
R indices (all data)	R1 = 0.0551, wR2 = 0.1232
Largest diff. peak and hole	0.272 and -0.224 $e.Å^{-3}$

3.2 FT IR spectral analysis

From the vibrational spectrum of TMEDA4NP (†Fig. S2), it is observed that the characteristic N-H stretching vibration occurred at 3446 cm^{-1}. Slight broadening observed in this region, indicates the presence of hydrogen bonding interaction between N-H protons with the nitro and phenolic oxygen. As the phenolic O-H group is already ionized, the broad envelop expected is not seen in this region. The phenolic ring C-H stretching vibration appeared at 3052cm^{-1}. Peaks at 2992, 2957 and 2896 cm^{-1} were attributed to C-H stretching vibrations of the amine. The fine structure below 2896 cm^{-1} is due to N-H stretching vibrations involved in hydrogen bonding. The intense broad peak at 1586cm^{-1} was attributed to the N-H deformation. The asymmetric and symmetric stretching vibrations of the NO_2 group yielded intense peaks at 1476 and 1299cm^{-1}. The peak due to phenolic C-O stretching overlapped with the peak at 1299cm^{-1}. The amine C-N stretching vibration occurred at 1103 and 1021cm^{-1}. The phenolic ring C-H bending vibration yielded its peak at 844 cm^{-1}. The FT IR spectrum thus carries all features expected for the amine and 4-nitrophenol.

3.3 FT NMR studies

The one dimensional ^{1}H, ^{13}C and DEPT-135 NMR spectra of TMEDA4NP were recorded in CD_3CN solvent and the characteristic ^{1}H and ^{13}C resonances corresponding to phenolic and tetramethylethylenediamine moieties were identified. The unequivocal assignments of these signals were further made by advanced 2D NMR techniques like gradient enhanced Correlation Spectroscopy (COSY) and Heteronuclear Single Quantum Coherence (HSQC). Two dimensional COSY was employed to establish connectivity between all directly coupled protons. The one bond ^{1}H-^{13}C connectivity between all carbons directly attached to protons was established from

HSQC spectrum. ^{1}H, ^{13}C, DEPT-135, COSY and HSQC spectra of TMEDA4NP are provided in †Figs. S3 to S7. The complete assignments of both ^{1}H and ^{13}C signals of TMEDA4NP are given in Table 3. An important feature of the ^{1}H NMR spectrum of TMEDA4NP is the presence of NH peak occurring at δ 4.97 ppm (†Fig. S3). The occurrence of NH peak illustrates the protonation of TMEDA, resulting in the formation of TMEDA4NP.

Table 3. ^{1}H and ^{13}C Chemical shift values for TMEDA4NP in CD_3CN

.

Group	Chemical shift (δ, ppm)	
	^{1}H	^{13}C
CH_2	2.65	45.04
CH_3	2.35	55.78
NH	4.97	-
CH (2,2′)	6.77	127.32
CHO (1)	8.02	169.52

3.4 UV-Vis-NIR analysis

The UV-Vis-NIR absorption spectrum of TMEDA4NP crystal recorded in the transmittance mode is shown in Fig.5. It is apparent that the transmittance of the crystal is almost negligible in the UV region. At about 480 nm, a sharp rise in the transmittance is observed and is mainly attributed to π-π* transition of the phenol ring. Above 480 nm it has sufficient transparency and the absorption in the Visible and near IR region is negligible. For the NLO applications the crystal must be transparent in the visible and near IR region.[31]

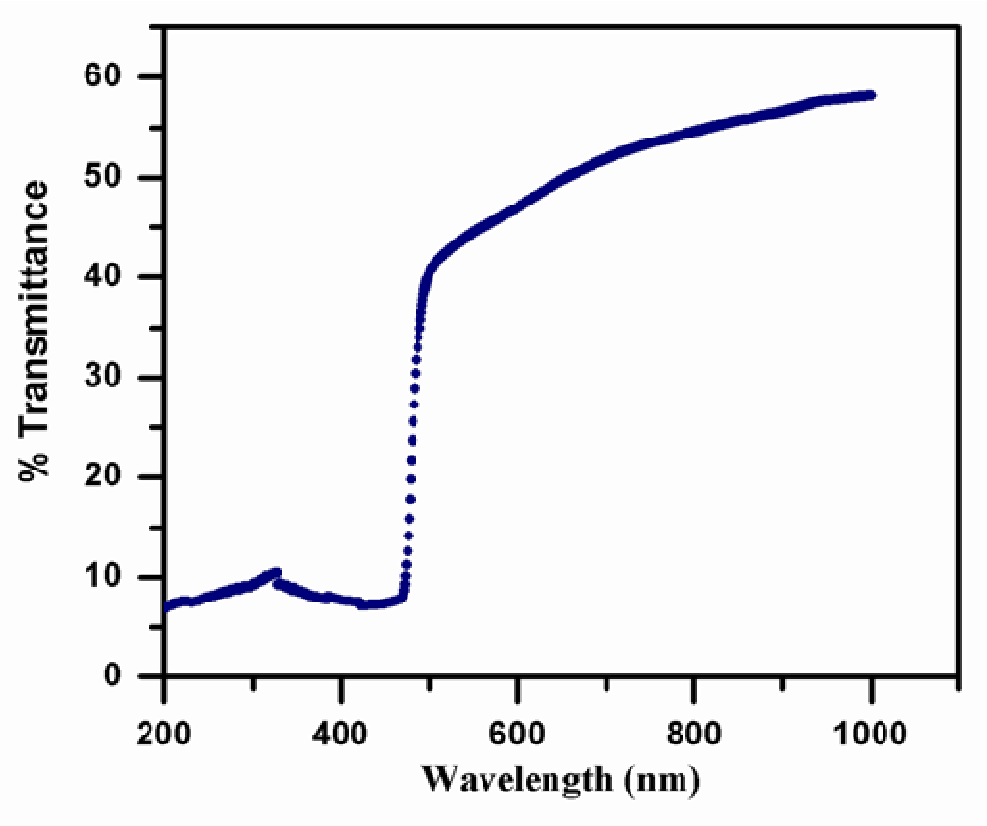

Fig. 5 UV-VIS-NIR Transmittance Spectrum of TMEDA4NP Crystal

3.5 Fluorescence analysis

Among the solid-state photo physical properties, fluorescence has attracted much interest in the field of optoelectronics.[32] The fluorescence spectrum of TMEDA4NP crystal with 380 nm excitation wavelength showed the emission maximum at 530 nm (Fig. 6). 4-nitrophenolate anionic moiety in the crystal acts as a fluorophore and is initially excited to any of the vibrational levels of the first electronic excited state, and brought down to levels close to S_1 by vibrational cascade, and then made to fluoresce at longer wavelength. The relatively higher value of the shift is attributed to the intermolecular hydrogen bonding interactions present in the crystal. The asymmetric nature of the emission spectrum illustrates the difference in the

interaction of the fluorescing moiety with the neighbors in the crystal, unlike in solutions. The fluorescent nature of the title compound also demonstrates the suitability of the TMEDA4NP for optoelectronic applications.

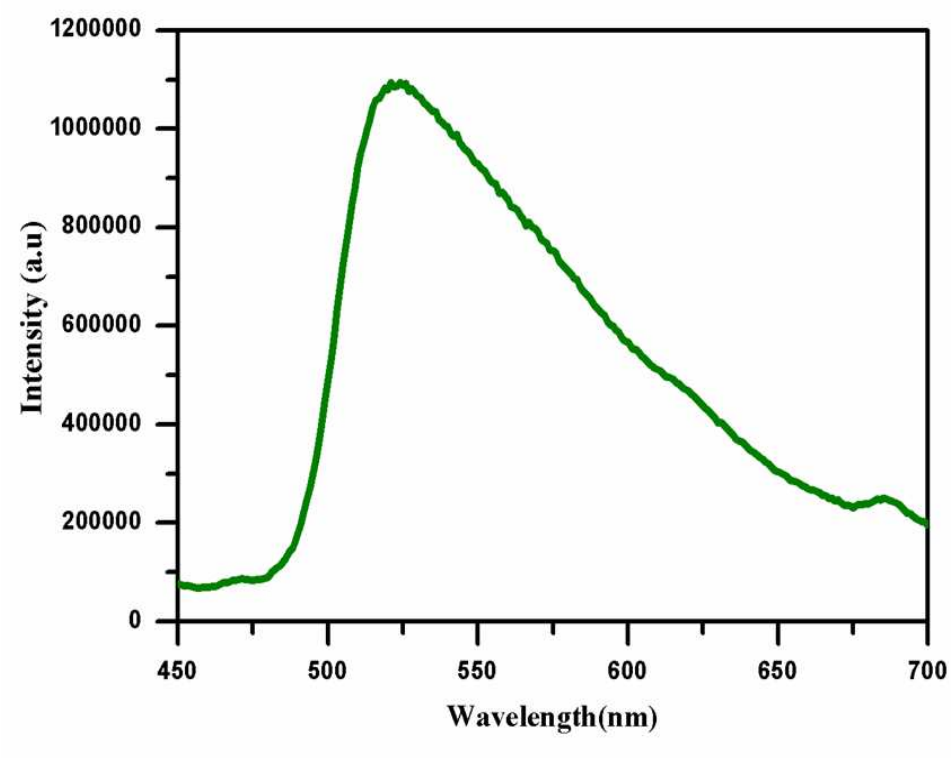

Fig. 6 Fluorescence emission of TMEDA4NP at 380 nm.

3.6 Thermal analysis

The thermogram obtained in the TGA study is illustrated in Fig. 7. The first derivative of the thermogram is also shown. The inflection point in the thermogram corresponds to the peak point in the derivative thermogram. From these traces, it is clear that an initial weight loss occurs at 121.8 ºC and a second major decomposition at 236.9 ºC. Thus, upon heat treatment at a heating rate of 10 ºC/min, TMEDA4NP undergoes a two-step decomposition process. Fig. 8 shows the result of the DSC study. From the DSC trace, it is evident that TMEDA4NP

undergoes phase transition (melting) at 118.9 ºC (T_{peak}) with an enthalpy change ΔH= 187 J/g. The melting point of the crystal determined using capillary tube method is in good agreement with the DSC results. The sharp feature of the DSC trace further confirms the absence of other impurities associated with TMEDA4NP crystal.

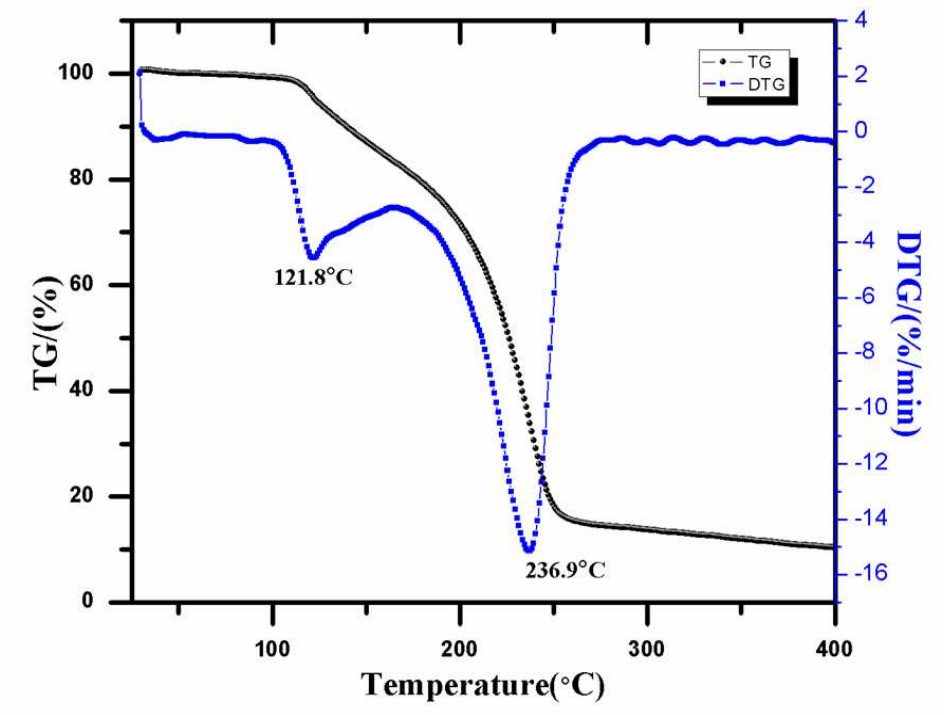

Fig. 7 TGA and DTG traces of TMEDA4NP

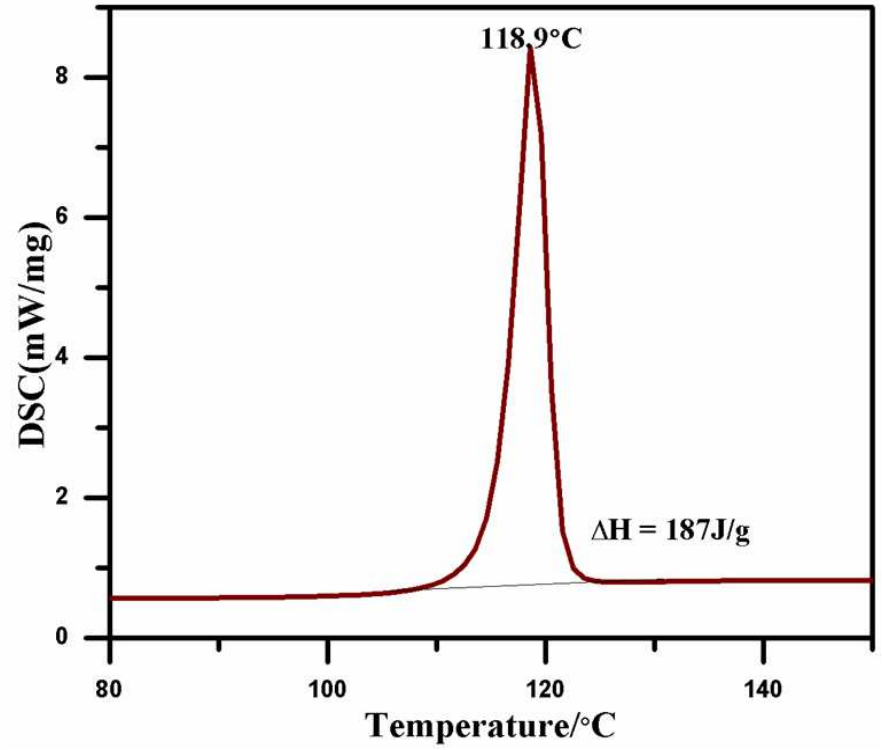

Fig. 8 DSC trace of TMEDA4NP showing the phase transition

3.7 Mechanical studies

The mechanical strength of any material is an integral parameter for the fabrication of devices and is strongly related to the structure and composition of the materials.[33] In this aspect, the Vicker's hardness number (H_v), was calculated from the Microhardness test using the following equation

$$H_v = \frac{1.8544P}{d^2} (Kg/mm^2) \quad (1)$$

where 'P' is the applied load in kg and 'd' is the diagonal length. The variation of hardness with load is shown in Fig. 9. The calculated H_v value for an applied load of 25 g was found to be

32 kg/mm^2 while that for an applied load of 30g, it was 34.5 kg/mm^2. From the hardness plot, it is clear that the hardness increases with the increase in load. This demonstrates that the grown crystal exhibits 'Reverse Indentation Size Effect' (RISE) property. It is also observed that the material gets damaged when the load is extended to 35g (insert of Fig.9) which is due to the release of the internal stress generated at the walls of the intender as well as the increase in depth of penetration of the intendentor.[34]

In order to study the nature of RISE more effectively, extensive set of other hardness parameter such as work hardening coefficient has been determined. According to the concept of Onstrich,[35] if the work hardening coefficient, $n < 1.6$, the lattice is hard and in such situations H_v decreases with increase in the load and the material will exhibit the Indentation Size Effect (ISE). On the other hand, in situations where $n > 1.6$, the lattice is soft and the material will exhibit RISE.[35] In the present case, the work hardening coefficient of TMEDA4NP is evaluated to be of 2.4, which is a clear indication of its softness.

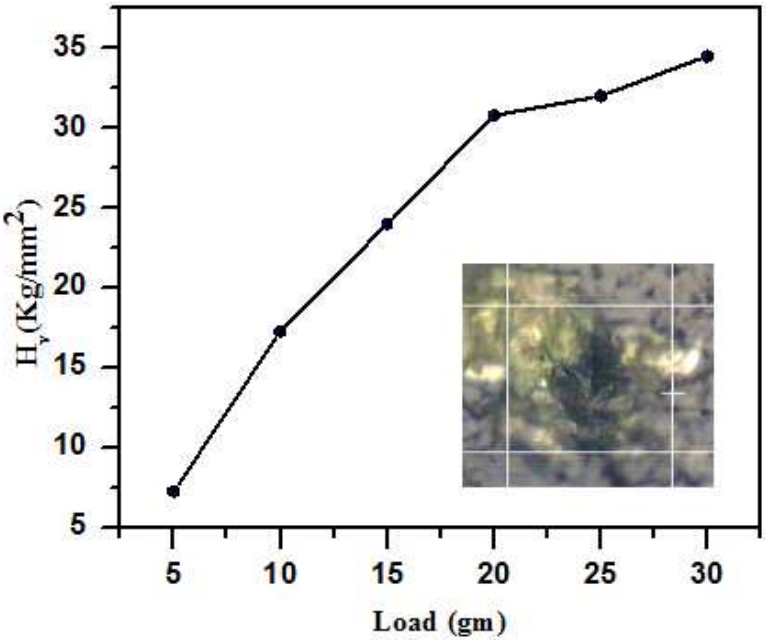

Fig. 9 Plot of Load with H_v of TMEDA4NP
Insert: Impression of the indentation mark at 35g load

3.8 Etching studies

Etch pattern of (100) plane as a function of time is shown Fig. 10. Elongated, oval shaped well defined etch pits were noticed on the surface of the crystal. The size of etch pits increased with the increase in the etching time. The time dependence of the growth of etch pits are attributed to the adsorption of reaction products formed as a result of the reaction between a crystal and the reactant.[36]Another notable observation is the consistency between the crystal symmetry and the shape of the etch pits. The occurrence of elongated etch pits is in well agreement with the two fold axes with glide plane normal to the b axis[37] observed in XRD studies.

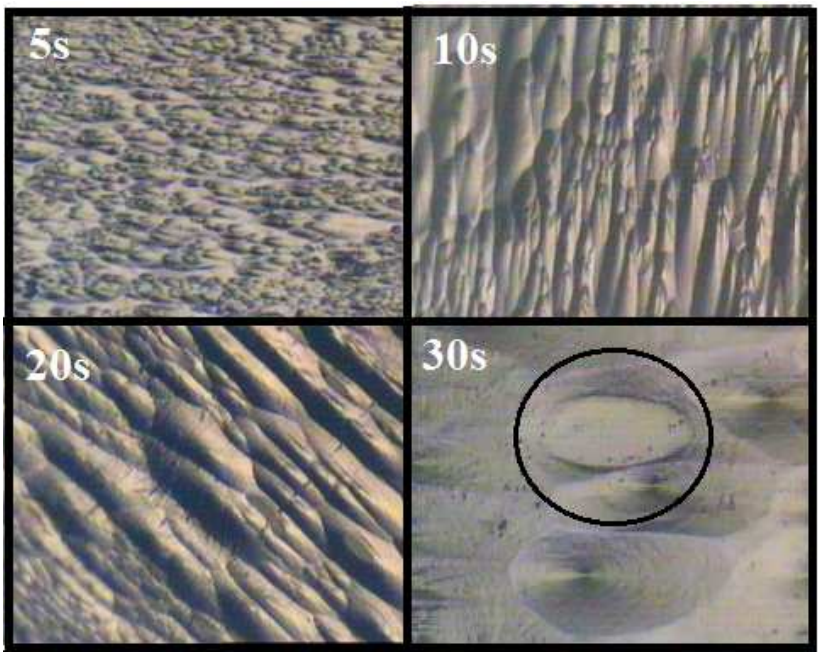

Fig. 10 Etch patterns of TMEDA4NP in acetonitrile etchant at different intervals

3.9 Nonlinear optical studies

Single beam Z scan technique is the most widely used method to study the third order nonlinear optical properties of materials because of its advantages such as high sensitivity and simplicity.[38] The open aperture (OA) Z-scan was employed to calculate the nonlinear optical absorption of TMEDA4NP. The OA curve of TMEDA4NP (Fig.11) demonstrates a strong reverse saturable absorption (RSA). In general, nonlinear optical absorption can be categorized in to two kinds (i) Saturable absorption (SA), where the transmittance of the sample increases with increasing optical intensity. (ii) Reverse saturable absorption (RSA) where the transmittance decreases while increasing the optical intensity. The later includes two photon absorption and multi-photon absorption.[39]

The single photon energy used in this experiment (2.33 eV) is less than that of the band gap energy (2.58 eV) of the TMEDA4NP crystal but greater than that of $E_g/2$ ($E_g/2<h\nu<E_g$), hence there is a possibility for two-photon absorption.

The normalized transmittance in the open aperture Z-scan experiment in the low irradiation limit for the Gaussian beam is given by Eq. (2) and is exploited to fit the open aperture curve

$$T(z) = 1 - \frac{2}{(x^2+9)(x^2+1)}\Delta\psi + \frac{4x}{(x^2+9)(x^2+1)}\Delta\varphi \qquad (2)$$

where, $\Delta\psi$ and $\Delta\varphi$ are on-axis phase shift due to nonlinear absorption and refraction respectively, $x = z/z_0$, in which z_0 ($= \pi\omega_0^2/\lambda$) is the Rayleigh range with ω_0 as the beam waist at the focus, and λ is pump wavelength. Generally, for open aperture z-scan, the refraction part is negligible and the nonlinear absorption plays a major role.

The first order nonlinear absorption coefficient (β) corresponding to the third-order nonlinear process is related to $\Delta\psi$ by

$$\beta = \frac{2\Delta\Psi}{I_0 L_{eff}} \qquad (3)$$

where I_o is input intensity and $L_{eff} = (1-\exp(-\alpha L))/\alpha$. α is the linear absorption coefficient and L is thickness of the sample.

The imaginary part of the third order nonlinear susceptibility $\chi^{(3)}$ is related to β and is calculated using the equation

$$\chi_{Im}^{(3)} = \frac{1}{3\pi} n_0^2 \varepsilon_0 c \lambda \beta \qquad (4)$$

Here, n_0 is the linear refractive index of medium, ε_0 is permittivity of the vacuum and c is velocity of light. From the OA curve, it is noticed that, at low input irradiance I_o = 1.6 GW/cm^2 there is no change in the transmittance i.e., the transmittance is independent of the input irradiance and further increase in the input intensity, at I_o = 31.6 GW/cm^2, there is a change in the transmittance ie., a reverse saturable absorption was observed. It is established that at higher input intensities there is a possibility to take either two photons (4.66 eV) or the excited state absorption is responsible for the observed reverse saturable absorption which leads to the optical limiting behavior.

OA Z scan profile of TMEDA4NP gives the value of imaginary part of the third order susceptibility 1.93×10^{-21}m^2/V^2. Generally, materials with an effective optical limiting properties display the so-called reverse saturable absorption (RSA).[40] From these observations, it is apparent that the grown TMEDA4NP crystal is a suitable candidate for optical limiting applications such as sensor protection (CCD, human eye *etc*).

3.10 Origin of nonlinear optical absorption in TMEDA4NP

TMEDA4NP possesses 4-nitrophenolate anion and TMEDA cation. The negative charge on the anion is delocalized by resonance over benzene and nitro group. This charge delocalization is the ultimate cause for its non-linear optical behavior. The band gap of TMEDA4NP is equal to 2.58 eV (480 nm) and for the NLO characterization, Nd:YAG laser of wavelength 532 nm was employed. Based on its NLO characteristics it is presumed that as a result of two photon absorption, the 4-nitrophenolate is raised to its virtual state (a short lived intermediate state) and then immediately excited to the first electronic excited state. In the present case the virtual state arises due to the distortion of electronic cloud as a consequence of input irradiance. This causes a large variation of the molecular dipoles upon laser excitation

which ultimately leads to the refractive and absorptive nonlinear optical responses. The presence of hydrogen-bonding interaction in TMEDA4NP could be the major cause for influencing the electron density distribution, luminescence and also two photon absorption. TMEDA4NP is thus a potential candidate for third order nonlinear optical applications.

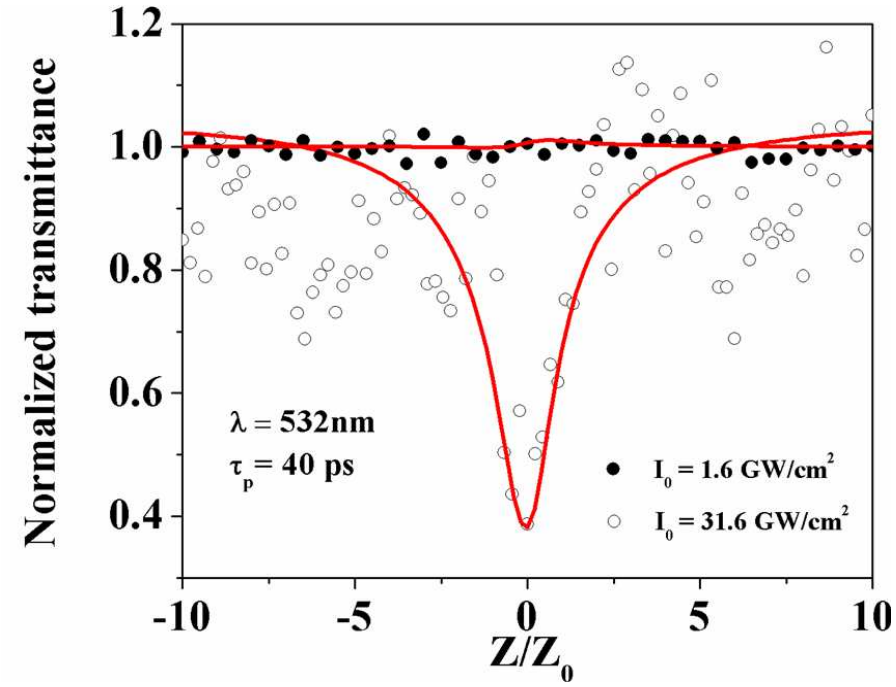

Fig. 11 Z scan curve of TMEDA4NP (open aperture)

4. Conclusion

This paper describes the self- assembled supramolecular structure of N,N,N′,N′-tetramethylethylenediammonium-bis-(4-nitrophenolate), a novel third order NLO crystal, synthesized using a single step protocol and grown from acetonitrile solvent. The self-assembled supramolecular structure of TMEDA4NP was elucidated from single crystal XRD analysis. Advanced spectroscopic techniques like UV-Vis-NIR and Fluorescence, FT-IR, FT-NMR were employed for determining its physiochemical properties. The crystal is transparent in the visible region between 480-1100nm. Thermal stability of the crystal was studied from TGA and the

phase transition was monitored by DSC. The fluorescence emission spectrum showed characteristic features of phenol moieties carrying delocalized electronic cloud. From the mechanical study, the softness of the material is established. Etching studies revealed the concurrence between the growth process and the crystal structure. Imaginary part of the third order susceptibility calculated using Z-scan studies showed that TMEDA4NP crystal exhibits good third order susceptibility, and also suitable for optical limiting applications. From the present investigation, it is concluded that both optical and mechanical properties of TMEDA4NP crystal relies entirely on its structure.

Acknowledgements

The authors are grateful to Professor Prem B Bisht and Mr. Sudhakar Reddy, Research Scholar, Department of Physics, IIT Madras for Z scan measurements and for fruitful discussions. The authors are also thankful to SAIF, IIT-Madras for supporting spectroscopic measurements. One of the authors Ms. P. Nagapandselvi acknowledges the Council of Scientific and Industrial research (CSIR), Government of India for funding the project.

Notes

† Electronic Supplementary Information (ESI) available: Experimental procedure, solubility determination of TMEDA4NP, Selected bond lengths and angles, hydrogen bond, Figures for hydrogen bonded network, FT IR, ^{1}H, ^{13}C, DEPT-135, COSY, and HSQC spectra.

CCDC No. : 900636.

Reference

1. J. L. Freeman, Q. Zhao, Y. Zhang, J. Wang, C. M. Lawsonb and G. M. Gray, *Dalton Trans.,* 2013, 42, 14281–14297.

2. C. F. Hernandez, G. R. Ortiz, S. Yen Tseng, M. P. Gaj and B. Kippelen, *J. Mater. Chem.,* 2009, 19, 7394-7401.

3. B. Gu, Y.H. Wang, X.C. Peng, J.P. Ding, J.L. He and H.T. Wang, *Appl. Phys. Lett.,* 2004, 85, 3687–3689.

4. R. D. Wampler, N.J. Begue and G.J. Simpson, *Cryst. Growth Des.,* 2008, 8, 2589-2594.

5. J.L. Bredas, C. Adant, P. Tackx and A. Persoons, *Chem. Rev.,* 1994, 94, 243-278.

6. D.S. Chemla and J. Zyss, Nonlinear Optical Properties of Organic Molecules andCrystals, *Academic Press., New York,* 1987.

7. D. R. Kanis , M.A. Ratner and T. J. Marks, *Chem. Rev.,* 1994, 94,195-242.

8. J. Zyss and J. F. Nicoudt, *Curr. Opin. Solid State Mater. Sci.,* 1996, 1, 533-546.

9. Z.-Yuan Li and Zi-Ming Meng, *J.Mater.Chem.,*2014, 2, 783-800.

10. C.H. Bosshard, K. Sutter, P.H. Pretre, J. Hulliger, M. Florsheimer, P. Kaat and P.Gunter, Organic Nonlinear Optical Materials, *Advances in Nonlinear Optics, vol. 1, Gordon and Breach, Amsterdam,* 1995.

11. C. Evans, M. B. Beucher, R. Masse and J. F.Nicoud, *Chem. Mater.,*1998, 10,847-854.

12. S.R. Marder, B. Kippelena, Alex K.-Y. Jen and N. Peyghambarian, *Nature.,* 1997, 388, 845- 851.

13. S. Draguta, M.S. Fonari, A. E. Masunov, J. Zazueta, S. Sullivan, M. Yu. Antipin and T.V. Timofeeva, *Cryst. Eng. Comm.,* 2013, 15, 4700-4710.

14. V. A. Russell, M. C. Etter and M. D. Ward, *Chem. Mater*,1994,6, 1206-1217.

15. J. Pecaut, J.P. Levy and T. Masse, *J. Mater. Chem.,* 1993, 3, 999-1003.

16. G. Gilli, and P. Gilli, The Nature of the Hydrogen Bond, *Oxford University Press.,2009,*163-167.

17. M. C. Etter, *Acc. Chem. Res.,*1990, 23, 120-139.

18. K.P. Glaser, A. Rachocki, P. Ławniczak, A. Ietraszko, C. Pawlaczyk, B. Hilczer and M. P. Michalska, *Cryst .Eng. Comm.,* 2013, 15, 1950-1959.

19. S. K. Callear, M. B. Hursthouse and T. L. Threlfall, *Cryst. Eng.Comm.,* 2010, 12, 898-908.

20. K. Clays, E. Hendrick, T.Verbiest and Andre Persoons, *Adv. Mater.,* 1998, 10, 643-655.

21. H. Koshima, Y. Wang and T. Matsuura, *Mol. Cryst. Liq. Cryst. Sci. Technol., Sect. A.,*1996, 63, 277-282.

22. M. S. Wong, C. Bosshard and P. Cunter, *Adv. Mater.,* 1997, 9, 837-842.

23. J. N. Sherwood, *Pure Appl. Opt.,* 1998, 7, 229-238.

24. K. Sangwal, *J. Cryst. Growth.,* 2002, 242, 215–228.

25. S.K. Sharmaa, S. Vermaa, B. B. Shrivastavab, V. K.Wadhawana, *J. Cryst. Growth.,* 2002, 244, 342-348.

26. Bruker (2004). APEX2, SAINT and SADABS. Bruker AXS Inc., Madison, Wisconsin, USA.

27. G. M. Sheldrick, Short history of SHELX , *Acta Crystallogr. SectA.,*2008, 64, 112-122.

28. M. Sheik-Bahae, A. Said, A, T. H . Wei, D. J. Hagan and E.W. Van Stryland, IEEE *J.Quantum Electr.,* 1990, 26, 760-769.

29. Y. Liu, H. Wang, H.Yi. Zhang, Li.H. Wang, *Cryst. Growth Des.,* 2005, 5, 231-235.

30. E. K. Anderson, I. G. Krogh Anderson and G. P. Sorensen, *Acta Chem. Scand*., 1989, 43, 624-635.

31. P. N. Prasad, *Springer Ser. Wave-Phenon.*, 1989, 9, 305-327.

32. Y.Ooyama, H. Egawa, T. Mamura and K. Yoshida, *Tetrahedron.,* 2008, 64 ,7219-7224.

33. W.A. Wooster, *Rep. Progr. Phys.,* 1953, 16, 62-82.

34. K. K. Bamzai, P. N. Kotru, B. M.Wanklyn, *J. Mater. Sci. Technol.,* 2000, 16, 405-410.

35. E. M. Onitsch, *Mikroscopia*.,1947, 2, 131-135.

36. K. Sangwal, Etching of crystals Theory*, Experiment and Applications* 1985.

37. A.B. Chase, R. Teviotdale, *J. Appl. Phys.,* 1968, 39, 3574-3577.

38. E.W. Van Stryland , M. Sheik-Bahae, G.; Kuzyk, *C.W. Dirk (Eds.),* 1998, 655-692.

39. Y.S. Zhou, E. S Wang, J.Peng, J. Liu, C.W. Hu, R.D. Huang, X. You, *Polyhedron.*, 1999, 18, 1419-1423.

40. K. D. Choquette, L. McCaughan, and D. K. Misemer, *J. Appl. Phys.,* 1989, 66, 4387-4392.